Enhanced Wavelet-based Method for Modal Identification from Power System Ringdowns

José. L. Rueda, *Member, IEEE*, and István. Erlich, *Senior Member, IEEE*

***Abstract*--In this paper, a method to the analysis of low-frequency electromechanical oscillations (LFEOs) based on continuous wavelet transform (CWT) is presented. The complex Morlet CWT is employed to decouple power system ringdown signals into single oscillatory modes (OMs) in order to estimate their frequencies, damping ratios, relative amplitudes and phase shifts as well as to detect nonstationarities. End-effects of CWT may cause inaccurate estimation of relative amplitudes and phase shifts. To make up for this drawback, an optimization problem is formulated in a least-square sense. The method is applied to synthetic and simulated ringdown signals and results are contrasted to results from Prony analysis.**

***Index Terms*--Modal identification, small signal stability, power system ringdowns, continuous wavelet transform, optimization.**

I. Introduction

THE occurrence of troublesome LFEOs has led to renewed emphasis on the study of the characteristics of OMs. Examples of small signal stability problems associated to poorly damped inter-area oscillations (with frequencies typically in the range of 0.2 to 0.8 Hz) are documented in several papers for different case histories including instances that have occurred in recent years in the Mexican power system [1], and the Pakistani power system [2].

The estimation of modal parameters associated to critical OMs have been accomplished either by using model-based methods (e.g. eigenanalysis from the perspectives of linear-analysis techniques [3], and the Normal Forms method [4]) or measurement-based techniques. Model-based methods are considered off-line methods, since they depend on approximate data and modeling processes. By contrast, measurement-based methods rely on actual response of a power system (i.e. signal records obtained from system measurements or from time domain simulations). Thus, these methods are of interest for monitoring LFEOs in real time [5].

As discussed in [6]-[8], typical measurement data can be classified into three typical categories: i) ringdown, ii) ambient, and iii) probing. Ringdown data occurs when the system is excited by some large disturbance, (e.g. adding/removing large loads, generator tripping, severe short circuits), and results in a transient response that can be easily observed and distinguished from ambient noise. This transient is usually assumed to be a sum of several damped sinusoids [6]. Ambient data is related to the fact that load switching throughout the day, which is random in nature, is persistently exciting the power system. This disturbance commonly appears as noise with very small magnitudes, and hence they cannot be easily distinguished from measurement noise [7]. Probing data is obtained when low-level pseudo-random noise is intentionally injected into the system for testing its performance [8].

There are several measurement-based methods that can be applied to extract modal parameters from power system ringdown signals. Among these are Prony analysis [9], the Steiglitz-McBride Algorithm [10], the Eigensystem Realization Algorithm [11], and Hilbert-Huang techniques [12]. The performances of the first three above-mentioned methods are compared in [13] with regard to accuracy of their identification. In [14], Prony Analysis and a method based on the Hilbert transform are compared in terms of measurement noise, calculation speed, accuracy, and the ability to discriminate between closely spaced modes. It was pointed out that Prony analysis is appropriate for ringdown data when linear and stationary signal portions are considered and is ineffective under noisy conditions. Hilbert transform based analysis can be employed to track the evolving dynamics of modal parameters. However, the ability of this approach to estimate modal parameters and to identify their temporal changes is obviated when applied to signals with multiple modal components since it cannot adequately distinguish two separate modes unless there is a large difference in either frequency or damping ratio [14].

The CWT constitutes an alternative mathematical tool for modal identification since its multi-resolution property is particularly useful for recognizing the features of a signal in both the time and frequency domains [15]. Several applications in civil and mechanical engineering has demonstrated its effectiveness in identifying natural frequencies and damping ratios in structural dynamic systems and vibrating systems [15], [16]. With regard to applications in power systems, past studies have focused on supervision of system disturbances [17], monitoring of system oscillations [18], and analysis of resonance phenomena in distribution networks [19]. However, further research is still needed for better exploitation of the wavelet transform concept in order to properly identify critical OMs. This paper presents a method that builds up on a previous work by the authors by employing the complex Morlet CWT in conjunction with an optimization problem in which the residual sum of the squared deviations

J. L. Rueda and I. Erlich are with the Institute of Electrical Power Systems, University Duisburg-Essen, Duisburg, Germany (e-mail: jose.rueda@uni-duisburg-essen.de, istvan.erlich@uni-due.de).

between a measured ringdown signal and a signal that is built on the basis of the CWT identification results is to be minimized. The key goal is to overcome adverse implications of end-effects of CWT on identification accuracy of modes' relative amplitudes and phase shifts.

The paper is organized into the following sections: Section II introduces some theoretical background about CWT and its usefulness in modal identification. Next, the proposed method is described in Section III. Test results are provided in Section IV. Finally, conclusions are given in Section V.

II. Background Theory

A. Continuous wavelet transform

The CWT of a continuous time signal f(t) is expressed by the following inner product in the Hilbert space [20]:

$$\mathrm{W_h f}(a,b)=\frac{1}{\sqrt{a}}\int_{-\infty}^{\infty}\mathrm{f}(t)\mathrm{h}^{*}\left(\frac{t-b}{a}\right)\mathrm{d}t \tag{1}$$

where a is a dilation or scaling factor, b is a translation or time shift factor, and $\mathrm{h}^{*}(t)$ is complex conjugate of a mother-wavelet function $\mathrm{h}(t)$.

It should be noted that the CWT is the sum over all time of the signal $\mathrm{f}(t)$ multiplied by scaled, shifted versions of the mother wavelet (i.e. the son wavelets). Hence, the CWT possesses localization properties in both time and frequency domains and consequently provides valuable information about $\mathrm{f}(t)$ at different levels of resolution and measures the similarity between $\mathrm{f}(t)$ and each son wavelet [21]. This indicates that the CWT can be employed for feature discovery by selecting a suitable mother-wavelet function. The mother-wavelet function constitutes a window function in both frequency and time domains [22]. Moreover, the ability of multi-resolution in the CWT can automatically filter out the noise from $\mathrm{f}(t)$, and thus no additional filters are needed [15].

B. Choice of the mother-wavelet

The effectiveness of CWT-based modal identification is strongly determined by proper choice of the mother wavelet function [23]. There are several different types of mother wavelet functions satisfying the admissibility condition, such as the Mexican hat, Gabor and Morlet, which can be selected according to the nature of the signal to be analyzed. It has been demonstrated that the complex Morlet wavelet is appropriate for the analysis of ringdown signals due to its capabilities in time-frequency localization for analytical signals [24]. This property is especially useful for modal identification purposes as demonstrated in several applications reported in civil and in mechanical engineering for the analysis of multi-degree of freedom systems [15], [16]. In this paper, the complex Morlet wavelet is formulated as shown below:

$$\mathrm{h}(t)=\mathrm{e}^{\mathrm{j}2\pi f_c t}\mathrm{e}^{-\frac{t^2}{f_b}} \tag{2}$$

where f_c is the wavelet central frequency parameter and f_b is a bandwidth parameter that controls the shape of the wavelet.

The Fourier transform of $\mathrm{h}(t)$ and its dilated form are given by

$$\hat{\mathrm{h}}(\omega)=\sqrt{2\pi}\mathrm{e}^{-\frac{(\omega-2\pi f_c)^2}{2}} \tag{3}$$

$$\hat{\mathrm{h}}(a\omega)=\sqrt{2\pi}\mathrm{e}^{-\frac{(a\omega-2\pi f_c)^2}{2}} \tag{4}$$

Note that $\hat{\mathrm{h}}(a\omega)$ is maximum at $a\omega=2\pi f_c$ and the complex Morlet wavelet can be considered as a linear bandpass filter whose bandwidth is proportional to 1/a or to the central frequency [25]. Besides, it can be interpreted that only the i-th oscillatory mode is strongly related to the scale $a=\frac{2\pi f_c}{\omega}$ [24].

The energy spectrum of $\mathrm{h}(t)$ is shown in Fig. 1 for a fixed f_c=0.2 Hz and for f_b equal to 2 and 10 Hz. Note that there is no zero frequency component when f_b=10, which implies that admissibility condition is satisfied. Besides, this indicates that an important value of f_b gives a narrower spectrum thus allowing a better resolution for the detection of low frequency OMs.

III. Proposed Method

A. First stage: CWT-based modal identification

Power system ringdown signals characterizing LFEOs can be represented mathematically by a sum of damped sinusoids, each one having the following form [26]:

$$x(t)=\mathrm{M}\mathrm{e}^{-\alpha t}\cos(\omega t+\theta)=\mathrm{A}(t)\left[\frac{\mathrm{e}^{j(\omega t+\theta)}+\mathrm{e}^{-j(\omega t+\theta)}}{2}\right] \tag{5}$$

where $\mathrm{A}(t)=\mathrm{M}\mathrm{e}^{-\alpha t}$ and t denotes time. The exponential decay constant α and the angular frequency ω correspond to the real and the imaginary components, respectively, of the i-th OM expressed as $s = \alpha+j\omega$. M is the mode relative amplitude and θ is the mode phase shift.

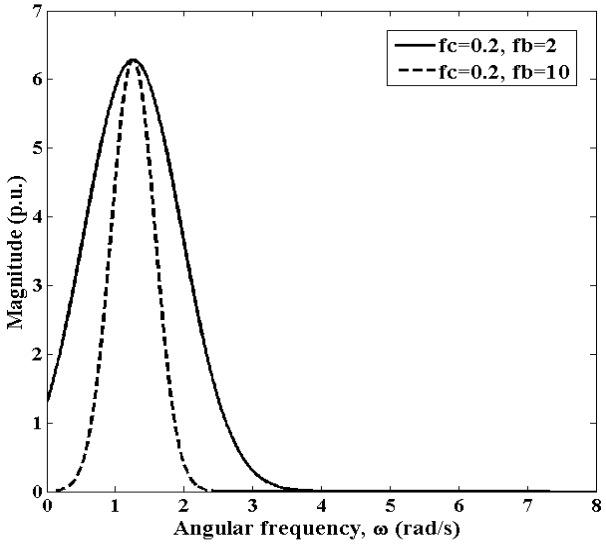

Fig. 1. Energy spectra of the complex Morlet wavelet.

By substituting (5) into (1), the Morlet CWT of $x(t)$ is expressed as

$$\mathrm{W_h}x(a,b)=\frac{1}{\sqrt{a}}\int_{-\infty}^{\infty}\mathrm{A}(t)\left[\frac{\mathrm{e}^{\mathrm{j}(\omega t+\theta)}+\mathrm{e}^{-\mathrm{j}(\omega t+\theta)}}{2}\right]\mathrm{h}^{*}\left(\frac{t-b}{a}\right)\mathrm{d}t \quad (6)$$

If the amplitude A(t) is expanded using Taylor series and then truncated at the first term around $t=b$ (i.e. the point where the son wavelet reaches its maximum), one can obtain

$$\mathrm{W_h}x(a,b)=\frac{\mathrm{M}}{\sqrt{a}}\int_{-\infty}^{\infty}\mathrm{e}^{-\alpha b}\left[\frac{\mathrm{e}^{\mathrm{j}(\omega t+\theta)}+\mathrm{e}^{-\mathrm{j}(\omega t+\theta)}}{2}\right]\mathrm{h}^{*}\left(\frac{t-b}{a}\right)\mathrm{d}t \quad (7)$$

By substituting $r=\dfrac{t-b}{a}$, $\mathrm{d}t = a\mathrm{d}r$ and substituting (2) into (7)

$$\mathrm{W_h}x(a,b)= \frac{\sqrt{a}\mathrm{M}\mathrm{e}^{-\alpha b}}{2}\int_{-\infty}^{\infty}\left[\mathrm{e}^{\mathrm{j}[\omega(ar+b)+\theta]}+\mathrm{e}^{-\mathrm{j}[\omega(ar+b)+\theta]}\right]\mathrm{e}^{-\mathrm{j}2\pi f_{\mathrm{c}}r}\mathrm{e}^{-\frac{r^2}{f_{\mathrm{b}}}}\mathrm{d}r \quad (8)$$

By completing the square on the exponential arguments in (8) and after solving the integral

$$\mathrm{W_h}x(a,b)=\frac{\sqrt{\pi a f_{\mathrm{b}}}\mathrm{M}\mathrm{e}^{-\alpha b}}{2}\left[\mathrm{e}^{-\frac{f_{\mathrm{b}}}{4}(2\pi f_{\mathrm{c}}-a\omega)^2+\mathrm{j}(b\omega+\theta)}+\mathrm{e}^{-\frac{f_{\mathrm{b}}}{4}(2\pi f_{\mathrm{c}}+a\omega)^2-\mathrm{j}(b\omega+\theta)}\right] \quad (9)$$

Let $\phi=\mathrm{j}(b\omega+\theta)+\pi a f_{\mathrm{b}}f_{\mathrm{c}}\omega$, then

$$\mathrm{W_h}x(a,b)=\frac{\sqrt{\pi a f_{\mathrm{b}}}\mathrm{M}\mathrm{e}^{-\alpha b}}{2}\mathrm{e}^{-\frac{f_{\mathrm{b}}}{4}\left[(2\pi f_{\mathrm{c}})^2+a^2\omega^2\right]}\left(\mathrm{e}^{\phi}+\mathrm{e}^{-\phi}\right) \quad (10)$$

If $\phi=\mathrm{j}(b\omega+\theta)+\pi a f_{\mathrm{b}}f_{\mathrm{c}}\omega$, then $\left|\mathrm{e}^{\phi}\right| >> \left|\mathrm{e}^{-\phi}\right|$ and $\mathrm{W_h}x(a,b)$ can be approximated by

$$\begin{aligned}\mathrm{W_h}x(a,b)&=\frac{\sqrt{\pi a f_{\mathrm{b}}}\mathrm{M}\mathrm{e}^{-\alpha b}}{2}\mathrm{e}^{-\frac{f_{\mathrm{b}}}{4}\left[(2\pi f_{\mathrm{c}})^2+a^2\omega^2\right]}\left(\mathrm{e}^{\phi}\right)\\&=\frac{\sqrt{\pi a f_{\mathrm{b}}}\mathrm{M}\mathrm{e}^{-\alpha b}}{2}\mathrm{e}^{-\frac{f_{\mathrm{b}}}{4}(a\omega-2\pi f_{\mathrm{c}})^2+\mathrm{j}(b\omega+\theta)}\end{aligned} \quad (11)$$

If the i-th OM related to the k-th scale gives a significant contribution to (11), the term $\mathrm{e}^{-\frac{f_{\mathrm{b}}}{4}(a\omega-2\pi f_{\mathrm{c}})^2}$ obtains its maximum at $a_{\mathrm{k}}=\dfrac{2\pi f_{\mathrm{c}}}{\omega}$, consequently

$$\mathrm{W_h}x(a,b)=\frac{\sqrt{\pi a f_{\mathrm{b}}}\mathrm{M}\mathrm{e}^{-\alpha b}}{2}\mathrm{e}^{\mathrm{j}(b\omega+\theta)} \quad (12)$$

By substituting t for b, (12) is rewritten in the form of time-varying amplitude and phase angle

$$\mathrm{W_h}x(a_k,t)=\frac{\sqrt{\pi a_{\mathrm{k}} f_{\mathrm{b}}}\mathrm{M}\mathrm{e}^{-\alpha t}}{2}\mathrm{e}^{\mathrm{j}(\omega t+\theta)} \quad (13)$$

Note that the real and the imaginary part of the i-th OM can be estimated from the logarithm of the modulus and the phase of the CWT, respectively. Thus

$$\ln\left|\mathrm{W_h}x(a_{\mathrm{k}},t)\right|=-\alpha t+\ln\left(\frac{\sqrt{\pi a_{\mathrm{k}} f_{\mathrm{b}}}\mathrm{M}}{2}\right) \quad (14)$$

$$\arg\left[\mathrm{W_h}x(a_{\mathrm{k}},t)\right]=\omega t+\theta \quad (15)$$

Subsequently, the real part, the imaginary part, the relative amplitude and phase shift of the i-th OM can be computed by applying linear regression analysis to a set of data given by $\left[\left(\mathrm{W_h}x\left(a_{\mathrm{k}},b_{\mathrm{l}}\right),b_{\mathrm{l}}\right),\cdots,\left(\mathrm{W_h}x\left(a_{\mathrm{k}},b_{\mathrm{m}}\right),b_{\mathrm{m}}\right)\right]$

$$\alpha=-\frac{\mathrm{m}\sum_{\mathrm{i}=1}^{\mathrm{m}}b_{\mathrm{i}}\ln\left|\mathrm{W_h}x\left(a_{\mathrm{k}},b_{\mathrm{i}}\right)\right|-\sum_{\mathrm{i}=1}^{\mathrm{m}}b_{\mathrm{i}}\sum_{\mathrm{i}=1}^{\mathrm{m}}\ln\left|\mathrm{W_h}x\left(a_{\mathrm{k}},b_{\mathrm{i}}\right)\right|}{\mathrm{m}\sum_{\mathrm{i}=1}^{\mathrm{m}}b_{\mathrm{i}}^2-\left(\sum_{\mathrm{i}=1}^{\mathrm{m}}b_{\mathrm{i}}\right)^2} \quad (16)$$

$$\omega=-\frac{\mathrm{m}\sum_{\mathrm{i}=1}^{\mathrm{m}}b_{\mathrm{i}}\arg\left|\mathrm{W_h}x\left(a_{\mathrm{k}},b_{\mathrm{i}}\right)\right|-\sum_{\mathrm{i}=1}^{\mathrm{m}}b_{\mathrm{i}}\sum_{\mathrm{i}=1}^{\mathrm{m}}\arg\left|\mathrm{W_h}x\left(a_{\mathrm{k}},b_{\mathrm{i}}\right)\right|}{\mathrm{m}\sum_{\mathrm{i}=1}^{\mathrm{m}}b_{\mathrm{i}}^2-\left(\sum_{\mathrm{i}=1}^{\mathrm{m}}b_{\mathrm{i}}\right)^2} \quad (17)$$

$$\mathrm{M}=\frac{2\mathrm{e}^{\frac{1}{\mathrm{m}}\left(\sum_{\mathrm{i}=1}^{\mathrm{m}}b_{\mathrm{i}}\ln\left|\mathrm{W_h}x\left(a_{\mathrm{k}},b_{\mathrm{i}}\right)\right|-\alpha\sum_{\mathrm{i}=1}^{\mathrm{m}}b_{\mathrm{i}}\right)}}{\sqrt{\pi a_{\mathrm{k}}f_{\mathrm{b}}}} \quad (18)$$

$$\theta=\frac{1}{\mathrm{m}}\left(\sum_{\mathrm{i}=1}^{\mathrm{m}}b_{\mathrm{i}}\arg\left|\mathrm{W_h}x\left(a_{\mathrm{k}},b_{\mathrm{i}}\right)\right|-\omega\sum_{\mathrm{i}=1}^{\mathrm{m}}b_{\mathrm{i}}\right) \quad (19)$$

The frequency and damping ratio of the i-th OM are given by $f=\dfrac{\omega}{2\pi}$, and $\zeta=\dfrac{-\alpha}{\sqrt{\alpha^2+\omega^2}}$, respectively.

It is worthwhile to mention that modal parameter changes can be detected by analyzing the slopes of logarithm of the modulus and phase of the CWT, since the straight line fits with $\ln\left|\mathrm{W_h}x(a_k,t)\right|$ and $\arg\left[\mathrm{W_h}x(a_k,t)\right]$ versus time can capture a mode damping change and a mode frequency change within a certain time window, respectively.

CWT-based analysis of a single-mode signal can be readily extended to multiple-mode signals by considering that CWT constitutes a time-frequency signal decomposition procedure that allows decoupling of signal individual modal components. The key idea is to choose a scaling factor a_k that maximizes the son wavelet, so that the frequency window covers only the mode associated with a_k while all the other modes and the signal noise are automatically filtered out. Also, for all modes of interest, the linear regression analysis is to be performed as well as for the single-mode signal case.

B. Second stage: Enhancement of identification accuracy

As discussed in Section II, the CWT works as a window function in both time and frequency domains. Time and frequency windows depend mainly on the center frequency parameter f_{c}, the bandwidth parameter f_{b}, the scaling factor a, and the translation factor b. Several guidelines are provided in a previous work by the authors for proper choice of these

parameters in order to estimate modal frequencies and damping ratios with reasonable accuracy [27].

Notwithstanding, by analyzing the convolution operation in (1) in light of the mother wavelet function in (2), it should be pointed out that, although the CWT is focused at a given time and represents the signal content in that vicinity, the window extends equally into the past and future [28]. The span of this analysis window depends on both the mother wavelet function and scale being analyzed, near the ends of the signal. Hence, the wavelet's analysis window may extend significantly beyond the length of data, deteriorating the identification accuracy (this phenomenon known as end-effect [15]), especially for mode relative amplitudes and phase shifts. To make up for this inadequacy, an optimization problem is formulated based on results from Morlet CWT-based modal identification as follows

$$\min \sum_{k=1}^{p} \left[x_{ms}(k\Delta t) - x(k\Delta t) \right]^2 \tag{20}$$

such that

$$M \geq 0, \; -\pi \leq \theta \leq \pi \tag{21}$$

where p is the number of samples, Δt is the sampling interval, x_{ms} is a measured ringdown signal, and x is a ringdown signal that is built using the preliminary estimated α, ω, M and θ, that is, (5) for single-mode signals whereas for multiple-mode signals x is given by

$$x(t) = \sum_{i=1}^{n} M_i e^{-\alpha_i t} \cos(\omega_i t + \theta_i) \tag{22}$$

The objective function in (20) considers only the adjustment of M and θ whereas α and ω are kept constant during the optimization since Morlet CWT-based modal identification provides good estimates for these parameters [27]. The optimization can be solved by using any standard optimization routine, such as, for instance, the fmincon function of Matlab's Optimization Toolbox.

IV. Test Results

Two different signal records are used to demonstrate the efficacy of the proposed method. For this purpose, several routines have been written in Matlab. Prony analysis is performed using the Dynamic System Identification Toolbox (DSI) [29].

A. Synthetic multi-mode signal

The proposed method is first applied to a three-mode synthetic ringdown signal with the following parameters:

Mode 1: $M_1 = 1.0$; $\theta_1 = 0$; $f_1 = 0.40$ Hz; $\zeta_1 = 3.6148$ %;
Mode 2: $M_2 = 0.7$; $\theta_2 = 30°$; $f_2 = 0.60$ Hz; $\zeta_2 = 5.30$ %;
Mode 3: $M_3 = 0.4$; $\theta_3 = 45°$; $f_3 = 1.10$ Hz; $\zeta_3 = 9.60$ %;

The sampling rate is 20 Hz. Additionally, a sudden detrimental change in damping (i.e. ζ_{New}=2.62 %) as well as a slight shift in modal frequency (i.e. f_{New}=0.38 Hz) was introduced to Mode 1 after 15 s in order to account for modal parameter changes. Fig. 2 shows a 30-s snapshot of the temporal evolution of the synthetic ringdown signal whereas the contour plot of its Morlet CWT magnitude is shown in Fig. 3 for a range of scales between 2 and 30. It is pointed out that the f_c is approximated to be near the typical modal frequencies (e.g. 0.2 – 0.5 Hz) since the scalogram of the Morlet CWT of a signal with dominant LFEOs will produce relatively large wavelet coefficients at scales where the oscillation in the wavelet correlates best with the low frequency signal features. Moreover, Morlet wavelets with low values of f_c contain only a few significant oscillations within a Gaussian window. This improves the location detection capabilities of the Morlet CWT [25]. Besides, f_b is set to 25 since an important value of f_b provides a suitable resolution for the detection of low frequency oscillatory modes and also precludes non-fulfillment of the admissibility condition.

The Morlet CWT possesses three salient peaks at the scales 21, 14, and 7 as highlighted with dashed lines in Fig. 3. These peaks are taken as the scaling factors whose associated frequency windows cover each mode separately. This is reasonable since the spectrum of the analyzed signal will reach peaks in the neighborhood of the frequencies associated to those modes that are dominant in the signal. Each peak corresponds to that of the Morlet CWT. Thus, the frequency window associated with the choice of a_k will cover the neighborhood of the corresponding modal frequency. Besides, it is worth to mention that a relatively lightly damped system possesses the property that its frequency response is highly localized in a neighborhood of modal frequencies. This property indeed eases the selection of proper values of a_k. Inadequate values of a_k would prevent the application of (12). This situation, which is beyond the scope of this paper, may occur especially when considering heavily damped systems.

In addition, it is interesting to note that the highest peak is related to the most poorly damped 0.4 Hz mode. This indicates that the Morlet CWT is especially useful for identifying those dominant oscillatory modes that may constitute possible threats to power system security.

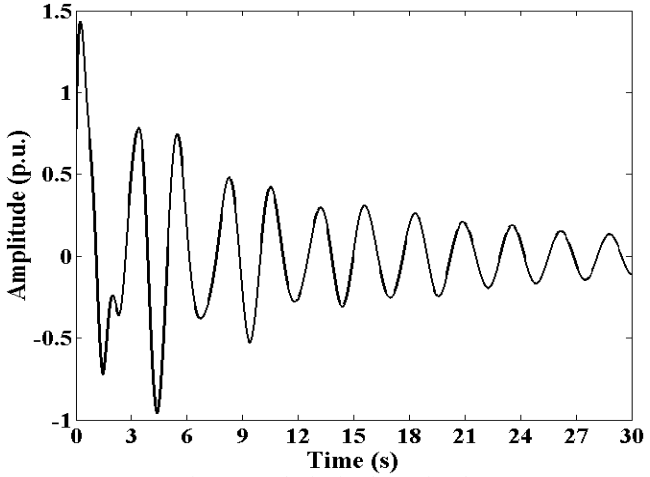

Fig. 2. Synthetic ringdown signal.

TABLE I
IDENTIFICATION OF MODAL PARAMETERS FOR THE SYNTHETIC TEST SIGNAL

Mode	a_k	Range of b (s)	Real				Estimates from Morlet CWT				Optimization	
			f (Hz)	ζ (%)	M (p.u.)	θ (deg)	f (Hz)	ζ (%)	M (p.u.)	θ (deg)	M (p.u.)	θ (deg)
1	21	7 - 10	0.4000	3.6148	1.0000	0.0000	0.3992	3.5988	6.6117	91.6160	0.9923	0.0020
2	14	7 - 10	0.6000	5.2977	0.7000	30.0000	0.6017	5.2584	4.4412	58.3959	0.6955	30.1454
3	7	4 - 7	1.1000	9.6012	0.4000	45.0000	1.1278	9.6342	3.9251	59.7079	0.4061	44.9416

The magnitude and phase plots of the Morlet CWT of the synthetic signal for the first mode with a_k=21 are illustrated in Fig. 4 and Fig. 5, respectively. Besides, the case with no detrimental changes in frequency and damping (i.e. without nonstationarities) is shown in both figures with black solid lines in order to show the tracking capability of Morlet CWT.

From Fig. 4, note that there is a change in the slope of the straight line segments of the logarithm of the CWT modulus at approximately t=15 s. This change corresponds to the above-mentioned damping decrement. Besides, a slight change is noticeable in the slope of the phase of the CWT depicted in Fig. 5 since only a slight variation in mode frequency has occurred. Based on (16) and (17), the new frequency and ζ of mode 1 are estimated by taking b in the range 19-24 s, which constitutes a range of positive small values where the plots of $\ln|W_h x(a_k,t)|$ and $\arg[W_h x(a_k,t)]$ versus t are approximately linear, since the time window in this range of contains the information of modal parameters. The identified frequency and ζ are 0.38 Hz and 2.57 %, which are quite close to f_{New} and ζ_{New} respectively. This demonstrates that Morlet CWT-based modal identification can be used not only to detect changes in modal frequencies and damping ratios, but also to accurately estimate what their new values might be.

Also, for the 15-s time window prior to the modal parameter changes, the frequency, ζ, relative amplitude and phase shift of each of the three modes are estimated based on (16) to (19). Subsequently, the initial estimated relative amplitudes and phase shifts are corrected by solving (20). The identification results are summarized in Table I, comparing with the above theoretical values. Final results from the integrated Morlet CWT-optimization method are highlighted with light gray. It can be seen that the sole application of Morlet CWT-Modal identification provides estimates of modal frequencies and damping ratios with an acceptable level of accuracy while it is no effective at all in terms of estimating relative amplitudes and phase shifts. The accuracy of relative amplitudes and phase shifts is significantly improved by solving the optimization problem as shown in the last two columns of Table I. Furthermore, although it is not shown in this paper for sake of brevity, it is worth to mention that, sensitivity analysis revealed that inaccurate estimates of mode parameters are obtained if the values of a_k are taken out of the ranges 19-23, 15-16, for modes 1 and 2 respectively, as well as different from 7 for mode 3. Indeed, this indicates that the accuracy of the Morlet CWT-based approach is more sensitive when estimating the parameters of less dominant modes.

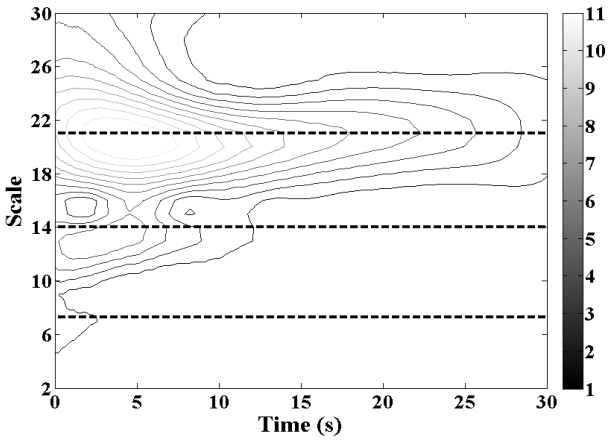

Fig. 3. Contour plot of the Morlet CWT magnitude for the synthetic ringdown signal with f_c=0.4, and f_b=25.

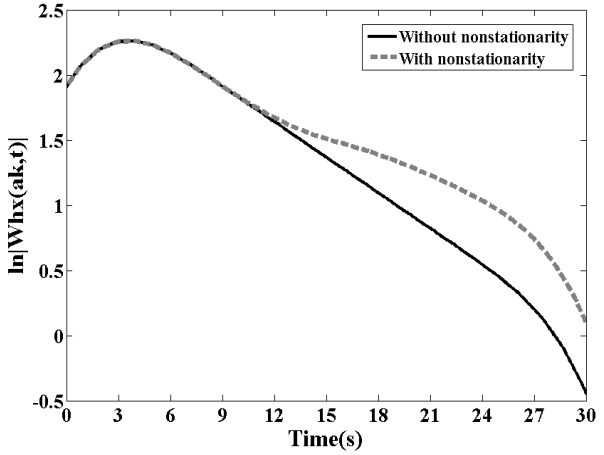

Fig. 4. Magnitude plot of the Morlet CWT for the synthetic ringdown signal with a_k=21, f_c=0.4, and f_b=25.

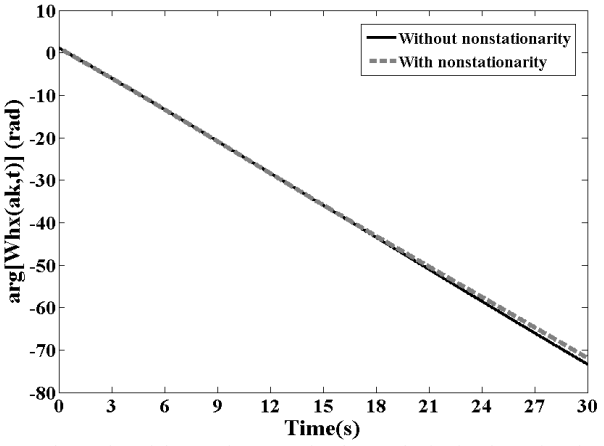

Fig. 5. Phase plot of the Morlet CWT for the synthetic ringdownsignal with a_k=21, f_c=0.4, and f_b=25.

TABLE II
TWO AREA-FOUR MACHINE POWER SYSTEM – IDENTIFIED MODAL PARAMETERS

Signal	Estimates from Prony analysis 6 – 10 s				Estimates from Morlet CWT 6 – 10 s			
	f (Hz)	ζ (%)	Normalized M (p.u.)	θ (deg)	f (Hz)	ζ (%)	Normalized M (p.u.)	θ (deg)
Pg1	0.6302	2.8210	0.7101	169.8572	0.6294	2.8340	0.7051	170.1354
Pg2	0.6302	2.8244	0.5750	167.3039	0.6303	2.8385	0.5657	167.5207
Pg3	0.6302	2.8268	1.0000	0.0000	0.6301	2.8702	1.0000	0.0000
Pg4	0.6303	2.8262	0.8936	-2.2200	0.6301	2.8671	0.8934	-2.1405

B. Simulated ringdown signal

The two area-four machine system shown in Fig. 6 is used to illustrate the application of the proposed method for identifying modal parameters of an inter-area mode from measured ringdowns. All generators are represented by subtransient model and equipped with static exciters, thermal turbines and governors, and power system stabilizers (PSSs). A detailed description of the system can be found in [30].

Due to its topology, the inter-area oscillation is easily induced by applying a step increase in load at bus 4 of 150 MW at 1.0 s. Time domain simulations are accomplished using the functions of the Power System Toolbox (PST) [30].

The Morlet CWT-optimization-based method is conducted on the four generators' active power output signals shown in Fig. 7. Results are summarized and compared to results from Prony analysis in Table II. Since Prony analysis and Morlet CWT-optimization-based method have significant differences arising from the underlying mathematical basis, M has been normalized by the value for generator 3 in order to allow for valid comparisons. As seen in the Table, phase shifts of generators 1 and 2 are nearly equal and in antiphase with those of generators 3 and 4, thus indicating an inter-area mode, in which the generating units in Area 1 oscillate against those in Area 2. Note also that normalized estimates from Morlet CWT-optimization-based method approximate very closely to those from Prony, therefore confirming the efficiency of the proposed method.

V. DISCUSSION

The proposed Morlet CWT-optimization-based method constitutes a viable tool for modal identification, which can be contrasted somehow with Fourier transform based methods. In this connection, it is worth to highlight some salient features of both approaches:

- A Fourier transform based approach transforms the view of the signal from time-based to frequency-based, which entails losing time information [31]. Thus, this approach is rather suitable for those signals whose properties do not change much over time (i.e. stationary signals).
- A Short-time Fourier transform based approach provides a sort of compromise between the time- and frequency-based views of a signal. Thus, some information about both when and at what frequencies a signal event occurs can be captured. Nevertheless, the accuracy of the obtained information is determined by the size of the window. Hence, its main drawback is that once a particular size of the time window is chosen, that window is the same for all frequencies [32].
- Morlet CWT is more effective in monitoring signal nonstationarities, since it is a variable-sizing technique which entails the ability to perform the so-called local analysis by allowing the use of long time intervals for capturing low-frequency information and shorter time windows for high-frequency information (i.e. time-frequency description of the signal).

VI. CONCLUSIONS

Two different signal records are used to demonstrate the efficacy of the proposed method. For this purpose, several A method for estimating modal parameters from power system ringdown signals is presented. The method is fundamentally based on the time-frequency characteristics of the Morlet CWT, which is used to estimate the frequencies, damping ratios, relative amplitudes and phase associated to dominant OMs. Adverse implications of end-effects of CWT on identification accuracy are overcome by employing the Morlet CWT in conjunction with an optimization problem that is formulated in a least-square sense. The efficiency of the proposed method has been demonstrated by using synthetic and simulated ringdown signals. The method constitutes a good alternative to the modal identification problem since modal parameters can be estimated to be as correct as those from Prony analysis. The ability of the method to detect changes of modal frequencies and damping ratios is also an additional attractive feature. Although not demonstrated in this work, it is worth to mention that, compared to Prony analysis, the employment of CWT in modal identification may lead to reduced computation time [19].

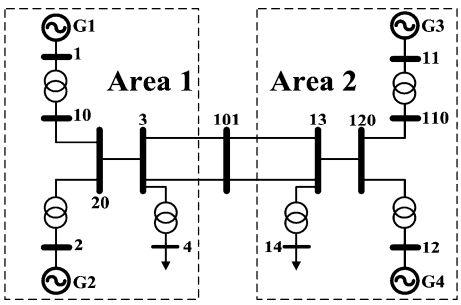

Fig. 6. Two area – four machine system.

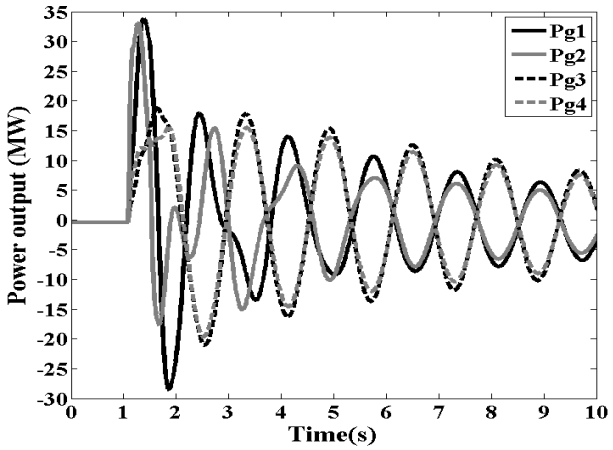

Fig. 7. Two area – four machine system. Generator active powers

VII. REFERENCES

[1] J. G. Flores, D. L. Rodríguez, O. M. Hoppe, G. Villa, F. S. Tello, G. C. Navarro, C. M. Román, and A. G. Terrones, " Damping of unstable low frequency oscillations through power system stabilizer tuning in the Mexican power system," in *Proc. 2007 CIGRE XII Iberian-American Regional Meeting*.

[2] M.W., Younas, and S.A. Qureshi, " Analysis of blackout of National Grid System of Pakistan in 2006 and the application of PSS and FACTS controllers as remedial measures," in *Proc. 2007 International Conference on Electrical Engineering*, pp. 1-6.

[3] L. Grigsby, *Power system stability and control*, Boca Raton: Taylor & Francis Group, 2007.

[4] J.J. Sanchez-Gasca, V. Vittal, M.J. Gibbard, A.R. Messina, D.J. Vowles, S. Liu, and U.D. Annakkage, " Analysis of higher order terms for small signal stability analysis," in *Proc. 2005 IEEE Power Engineering Society General Meeting,*, Vol. 2, pp. 1745 - 1753.

[5] J.F. Hauer, D.J. Trudnowski, and J.G. DeSteese,, " A Perspective on WAMS Analysis Tools for Tracking of Oscillatory Dynamics," in *Proc.2007 IEEE Power Engineering Society General Meeting,*, pp. 1-10.

[6] D.J. Trudnowski, and J.W. Pierre, "Overview of Algorithms for Estimating Swing Modes form Measured Responses," in *Proc. 2009 IEEE Power & Energy Society General Meeting*, pp. 1-8.

[7] H. Ghasemi, "On-line monitoring and oscillatory stability margin prediction in power systems based on system identification," Ph.D. dissertation, University of Waterloo, Canada, 2006.

[8] N. Zhou, D.J. Trudnowski, J.W. Pierre, and W.A. Mittelstadt, "Electromechanical Mode Online Estimation Using Regularized Robust RLS Methods," *IEEE Transactions on Power Systems*, vol. 23, no. 4, pp. 1670 – 1680, Nov. 2008.

[9] J.F. Hauer, "Application of Prony analysis to the determination of modal content and equivalent models for measured power system response," *IEEE Transactions on Power Systems,*, vol. 6, no. 3, pp. 1062-1068, Aug. 1991.

[10] K. Steiglitz, and L. McBride, "A technique for the identification of linear systems," *IEEE Transactions on Automatic Control*, vol. 10, no. 4, pp. 461-464, Oct 1965.

[11] J. Juang, and R. S. Pappa, "An eigensystem realization algorithm for modal parameter identification and model reduction," *Journal of Guidance and Control*, vol. 8, no. 5, pp. 620-627, Sept.-Oct. 1985.

[12] A.R. Messina, and V. Vittal, "Nonlinear, non-stationary analysis of interarea oscillations via Hilbert spectral analysis," *IEEE Transactions on Power Systems*, vol. 21, no. 3, pp. 1234-1241, Aug. 2006.

[13] J.J. Sanchez-Gasca, and J.H. Chow, "Performance comparison of three identification methods for the analysis of electromechanical oscillations," *IEEE Transactions on Power Systems*, vol. 14, no. 3, pp. 995 – 1002, Aug. 1999.

[14] T. J. Browne, V. Vittal, G. T. Heydt, and A. R. Messina, "A comparative assessment of two techniques for modal identification from power system measurements," *IEEE Transactions on Power Systems*, vol. 23, no. 3, pp. 1408 – 1415, Aug. 2008.

[15] S. Chen, J. Liu, and H. Lai, "Wavelet analysis for identification of damping ratios and natural frequencies," *Journal of Sound and Vibration*, vol. 323, no. 1, pp. 130-147, March 2009.

[16] J. Lardies, and S. Gouttebroze, " Identification of modal parameters using the wavelet transform," *International Journal of Mechanical Sciences*, vol. 44, no. 11, pp. 2263-2283, Nov. 2002.

[17] S. Huang, C. Hsieh, and C. Huang, "Application of Morlet wavelets to supervise power system disturbances," *IEEE Transactions on Power Delivery*, vol. 14, no. 1, pp. 235 – 243, Jan.1999.

[18] S. Bruno, M. De Benedictis, and M. La Scala, " Taking the pulse of Power Systems: Monitoring Oscillations by Wavelet Analysis and Wide Area Measurement System," in *Proc. 2006 IEEE PES Power Systems Conference and Exposition*, pp. 436 – 443.

[19] K. Hur, and S. Santoso, "Estimation of System Damping Parameters Using Analytic Wavelet Transforms," *IEEE Transactions Power Delivery*, vol. 24, no. 3, pp. 1302-1309, July 2009.

[20] S. Mallat,, *A Wavelet Tour of Signal Processing*. San Diego: Academic Press, 1998.

[21] W. J. Staszewski, "Identification of Damping in MDOF systems using Time-scale Decomposition," *Journal of Sound and Vibration*, vol. 203, no. 2, pp. 283-305, June 1997.

[22] J. C. Goswami, and A. K. Chan, *Fundamentals of Wavelets: Theory, Algorithms, and Applications*. New York: John Wiley & Sons, 1999.

[23] P. Kang, and G. Ledwich, "Estimating power system modal parameters using wavelets," in *Proc. 1999 Fifth International Symposium on Signal Processing and its Applications*, pp. 563-566.

[24] B.F. Yan, A. Miyamoto, and E. Brühwiler, "Wavelet Transform-based Modal Parameter Identification Considering Uncertainty," *Journal of Sound and Vibration*, vol. 291, no. 1-2, pp. 285-301, March 2006.

[25] P. S. Addison, J. N. Watson, and T. Feng, "Low-Oscillation Complex Wavelets," *Journal of Sound and Vibration*, vol. 254, no. 4, pp. 733-762, July 2002.

[26] A.R. Messina, *Inter-area Oscillations in Power Systems*. New York: Springer, 2009.

[27] J. L. Rueda, C. A. Juárez, and I. Erlich, "Wavelet-based Analysis of Power System Low-Frequency Electromechanical Oscillations," [Online]. IEEE Transactions on Power Systems, Feb. 2010.

[28] T. Kijewski, and A. Kareem, "On the Presence of End Effects and Associated Remedies for Wavelet-Based Analysis" *Journal of Sound and Vibration,* vol. 256, no. 5, pp. 980-988, 2002.

[29] BPA/PNNL. Dynamic System Identification Toolbox. [Online]. Available: ftp://ftp.bpa.gov/pub/WAMS_Information/

[30] J. Chow, and G. Rogers. Power system toolbox version 3.0, Ontario: Cherry Tree Scientific Software, 2008. [Online]. Available: http://www.eagle.ca/~cherry/

[31] K.K.-P. Poon, and K.-C. Lee, "Analysis of transient stability swings in large interconnected power systems by Fourier transformation", *IEEE Transactions on Power Systems*, Vol. 3, No. 4, Nov. 1988, pp. 1573 – 1581.

[32] P. O'Shea, "The use of sliding spectral windows for parameter estimation in power system disturbance monitoring", *IEEE Transactions on Power Systems*, Vol. 15, No. 4, Nov. 2000, pp. 1261 – 1267.

José L. Rueda (M'07) was born in 1980. He received the Electrical Engineer diploma from the Escuela Politécnica Nacional (EPN), Quito, Ecuador, in 2004, and the Ph.D. degree in electrical engineering from the Universidad Nacional de San Juan, San Juan, Argentina, in 2009. From September 2003 till February 2005, he worked in Ecuador, in the fields of industrial control systems and electrical distribution networks operation and planning. Currently, he is pursuing postdoctoral research at the Institute of Electrical Power Systems (EAN, by the acronym in German), as a part of a one-year scholarship financed by the University Duisburg-Essen. His current research interests include power system stability and control, system identification, power system planning, probabilistic and artificial intelligent methods, and wind power.

István Erlich (SM'08) was born in 1953. He received the Dipl.-Ing. degree in electrical engineering and the Ph.D. degree from the University of Dresden, Dresden, Germany, in 1976 and 1983, respectively. After his studies, he worked in Hungary in the field of electrical distribution networks. From 1979 to 1991, he was with the Department of Electrical Power Systems of the University of Dresden. In the period of 1991 to 1998, he worked with the consulting company EAB, Berlin, Germany, and the Fraunhofer Institute IITB Dresden, respectively. During this time, he also had a teaching assignment at the University of Dresden. Since 1998, he has been a Professor and head of the Institute of Electrical Power Systems at the University of Duisburg-Essen, Duisburg. Germany. His major scientific interest is focused on power system stability and control, modelling, and simulation of power system dynamics, including intelligent system applications. Dr. Erlich is a member of VDE and the chairman of the IFAC (International Federation of Automatic Control) Technical Committee on Power Plants and Power Systems.